Development of a Reverse Genetic System for Infectious Salmon Anemia Virus: Rescue of Recombinant Fluorescent Virus by Using Salmon Internal Transcribed Spacer Region 1 as a Novel Promoter

Daniela Toro-Ascuy,[a] Carolina Tambley,[a] Carolina Beltran,[a] Carolina Mascayano,[b] Nicolas Sandoval,[a] Eduardo Olivares,[a] Rafael A. Medina,[c] Eugenio Spencer,[d] Marcelo Cortez-San Martín[a]

Laboratorio de Virología Molecular, Centro de Biotecnología Acuícola (CBA), Facultad de Química y Biología, Universidad de Santiago de Chile, Santiago, Chile[a]; Laboratorio de Simulación Molecular, Departamento de Ciencias del Ambiente, Facultad de Química y Biología, Universidad de Santiago de Chile, Santiago, Chile[b]; Laboratory of Molecular Virology, Departamento de Infectología e Inmunología Pediátrica, Escuela de Medicina, Millennium Institute on Immunology and Immunotherapy, Pontificia Universidad Católica de Chile, Santiago, Chile[c]; Laboratorio de Virología, Centro de Biotecnología Acuícola (CBA), Facultad de Química y Biología, Universidad de Santiago de Chile, Santiago, Chile[d]

Infectious salmon anemia (ISA) is a serious disease of marine-farmed Atlantic salmon (*Salmo salar*) caused by ISA virus (ISAV), belonging to the genus *Isavirus*, family *Orthomyxoviridae*. There is an urgent need to understand the virulence factors and pathogenic mechanisms of ISAV and to develop new vaccine approaches. Using a recombinant molecular biology approach, we report the development of a plasmid-based reverse genetic system for ISAV, which includes the use of a novel fish promoter, the Atlantic salmon internal transcribed spacer region 1 (ITS-1). Salmon cells cotransfected with pSS-URG-based vectors expressing the eight viral RNA segments and four cytomegalovirus (CMV)-based vectors that express the four proteins of the ISAV ribonucleoprotein complex allowed the generation of infectious recombinant ISAV (rISAV). We generated three recombinant viruses, wild-type rISAV$^{901\_09}$ and rISAVr$^{S6-NotI-HPR}$ containing a NotI restriction site and rISAV$^{S6/EGFP-HPR}$ harboring the open reading frame of enhanced green fluorescent protein (EGFP), both within the highly polymorphic region (HPR) of segment 6. All rescued viruses showed replication activity and cytopathic effect in Atlantic salmon kidney-infected cells. The fluorescent recombinant viruses also showed a characteristic cytopathic effect in salmon cells, and the viruses replicated to a titer of 6.5×10^5 PFU/ml, similar to that of the wild-type virus. This novel reverse genetics system offers a powerful tool to study the molecular biology of ISAV and to develop a new generation of ISAV vaccines to prevent and mitigate ISAV infection, which has had a profound effect on the salmon industry.

Infectious salmon anemia (ISA) is a disease that principally affects Atlantic salmon (*Salmo salar*), which has caused enormous losses to salmon farming worldwide (1, 2). ISA was first reported in 1984 in Norway (3) and subsequently was identified in Canada (4), Scotland (5), the United States (6), the Faroe Islands (Denmark) (6), and Chile (7). The etiological agent of this disease is the infectious salmon anemia virus (ISAV), a pleomorphic enveloped virus with a diameter of 45 to 140 nm, which belongs to the family *Orthomyxoviridae* (8). Its genome has 8 negative-polarity single-stranded RNA (ssRNA) segments that encode 10 proteins. Sequence similarity analyses of the genomes of different ISAV isolates show significant variation in the coding regions. In contrast, the untranslated regions (UTR) at both ends of each segment are highly conserved (9–11), as has been described for other orthomyxoviruses as well (e.g., influenza A and B viruses) (12).

There is little knowledge at present about the functions of the ISAV proteins. Bioinformatic analyses of the sequences predict that segments 1, 2, and 4 encode the subunits of the RNA-dependent RNA polymerase (RdRp), analogous to PB2, PB1, and PA, respectively, of the influenza A virus. Segment 3 encodes the nucleoprotein (NP), which has been reported to have the capacity to bind ssRNA (13). For influenza virus, it has been shown that these four proteins are associated with the eight segments of the viral RNA to form ribonucleoprotein complexes (RNPCs) (14). These eight RNPCs are the smallest infectious units required to initiate viral replication (14). Segment 5 encodes the fusion protein (F), which has been shown to be present on the surface of the viral

membrane and allows the fusion of the membrane of the viral particle with the cellular endosome in the first stages of infection, resulting in the release of the RNPCs to the cytoplasm (15). Segment 6 encodes the hemagglutinin-esterase (HE) protein, which is also present on the viral surface and whose function is to bind sialic acid residues of the cellular receptor (16). The HE protein also presents receptor-destroying enzyme activity that favors the release of new viral particles that emerge from the cellular membrane (17). In contrast to what is observed in the hemagglutinin of the influenza A virus, in which the stalk region is highly conserved, it has been reported that the ISAV HE protein has a highly variable region toward the carboxyl terminus near the transmembrane re-

gion, called the highly polymorphic region (HPR) based on its high degree of polymorphism (18). The HPR encodes 35 amino acids, and approximately 30 variants have been reported in Europe, North America, and Chile (19–21). It has been postulated that this is due to a deletion phenomenon based on an ancestral strain with a longer HPR, named HPR0 (22). The first HPR0 strain that did not present clinical signs of ISA was identified in Scotland in wild salmon and was catalogued as avirulent (23). In contrast, strains that have deletions in this region are capable of producing clinical signs associated with a virulent phenotype of ISAV. Segment 7 encodes nonstructural proteins analogous to NS1 and NS2 of the influenza A virus (24). Finally, segment 8 encodes a transcript that contains two overlapping open reading frames (ORFs). ORF1 encodes the matrix protein (M), while ORF2 encodes the M2 protein, which has been shown to be involved in modulating the response of type I interferon (IFN) together with the NS1 protein (25).

The detailed study of the influenza virus has been possible thanks to the development of reverse genetic systems, which allow the manipulation of the viral genome. This has allowed us to determine virulence markers and pathogenic determinants of different viral strains, as well as to study the functions of viral proteins in detail (26). The most commonly used reverse genetic system for the influenza virus is based on cloned DNA plasmids that permit transcription of the 8 genomic RNAs under the command of the RNA polymerase I and the expression of the proteins that constitute the viral RNA polymerase and NP under the command of RNA polymerase II (27–29). Until now, there have been no reports of a successful reverse genetic system for ISAV. An important obstacle in generating such a system has been the lack of an efficient promoter for RNA polymerase I, which, until now, had not been described for the Atlantic salmon. As the promoters for RNA polymerase I are strictly species specific, they do not have a clear genetic structure and are found in the intergenic spacer (IGS) region of ribosomal RNAs (30). Identifying the sequences corresponding to the promoter for polymerase I and its enhancers is difficult, considering that the IGS region in the *Salmo* genus varies between 15 and 23 kb in length (31), highlighting the need for developing plasmid technologies that can be used routinely in fish cells.

There is an urgent need to understand the virulence factors and pathogenic mechanisms of ISAV. Thus, we sought to develop and implement a plasmid-based reverse genetic system to generate recombinant ISAV (rISAV) as a tool to study the molecular biology of this virus. Due to the need of a salmon species-specific promoter with the characteristics of RNA polymerase I, we evaluated the use of internal transcribed spacer region 1 (ITS-1) of 571 bp from *Salmo salar*, which has recently been described to contain transcription promoter and regulator motifs in flatworms (32). Here, we report the generation of the first reverse genetic system for ISAV based on plasmids containing the salmon ITS-1 region as a novel promoter element. This promoter proved to be key for establishing a rescue system that allowed the modification of the HPR of the HE protein (segment 6), which led to the generation an enhanced green fluorescent protein (EGFP)-labeled rISAV.

MATERIALS AND METHODS

Cell lines. Atlantic salmon kidney (ASK) cells (CRL-2747; ATCC) were cultured in Leibovitz medium (L-15; HyClone) supplemented with 50 μg/ml gentamicin, 10% fetal bovine serum (FBS; Corning Cellgro, Mediatech), 6 mM L-glutamine (Corning Cellgro, Mediatech), and 40 μM β-mercaptoethanol (Gibco, Life Technologies). The RTG-2 cells (ECACC 90102529), from rainbow trout gonad tissue, were cultured in minimal essential medium (MEM; HyClone) supplemented with 50 μg/ml gentamicin, 10% FBS, 10 mM L-glutamine, 1% nonessential amino acids (HyClone), and 10 mM HEPES (HyClone). The CSE-119 cells, from Coho salmon embryo (ECACC 95122019), were cultured in MEM supplemented with 50 μg/ml gentamicin, 10% FBS, 2 mM L-glutamine, and 1% nonessential amino acids. Cell lines were grown at 16°C, unless otherwise stated, without CO_2, with the exception of CSE-119, which required 5% CO_2.

Purification of ISAV particles. Virus was purified from 40 ml of culture supernatant from ASK cells on day 14 after infection with the ISAV901_09 strain. The supernatant was clarified at $1,000 \times g$ at 4°C for 20 min and then was ultracentrifuged at $133,200 \times g$ for 2 h at 4°C. The viral pellet was resuspended in 100 μl of TNE buffer (10 mM Tris-HCl, 0.1 M NaCl, 1 mM EDTA, pH 7.5) overnight at 4°C. The suspension was loaded in 4 ml of a sucrose cushion at 20% (wt/vol) in TNE buffer and ultracentrifuged at $124,200 \times g$ at 4°C for 2 h. Finally, the purified pellet was resuspended in 50 μl of TNE buffer.

vRNA extraction. Viral RNA (vRNA) was extracted from 50 μl of purified ISAV901_09 virus using the commercial E.Z.N.A. total RNA kit II (Omega, Bio-Tek, Inc.) according to the supplier's instructions. The purified RNA then was quantified and stored at −80°C until use.

Bioinformatic analysis and primer design for amplification of the viral genome of ISAV 901_09. Sequences were selected, including the noncoding 5′ and 3′ UTR ends of the eight genomic segments, from the publications of Fourrier et al., Kulshreshtha et al., and Merour et al. (10, 33, 34). The sequences were from two Scottish isolates (390/98 and 982/08) (33), a Norwegian isolate (Glesvaer/2/90) (10), two Canadian isolates (NBISA01 and RPC NB 98-049) (34), and one Chilean isolate (ADL-PM 3205 ISAV) (34). Multiple nucleotide (nt) alignments were made with the ClustalW2 program (http://www.ebi.ac.uk/Tools/msa/clustalw2/). Based on alignments made with the available sequences, universal primers were designed to amplify the complete ORF of the 8 viral segments and part of the 5′ and 3′ UTRs of any ISAV strain (Table 1 and Fig. 1). Thus, the full genome of the ISAV901_09 strain, except for the regions covered by the primers at the end of the 5′ and 3′ UTRs, was amplified and sequenced.

RT-PCR. The cDNA of the eight genomic segments was obtained by reverse transcription-PCR (RT-PCR) using the SuperScript OneStep RT-PCR system with platinum *Taq* DNA polymerase (Invitrogen) by following the supplier's instructions. The F (forward) and corresponding R (reverse) primers (10 μM) (Table 1) and 50 ng of viral RNA were used to amplify the cDNA of each segment. The cycle conditions used were 50°C for 30 min for the reverse transcription step, followed by 94°C for 2 min, and then 35 cycles of 94°C for 15 s, an annealing step of 52°C (segments 1a/1b and 6) or 49°C (segments 2 to 5 and 7 to 8) for 30 s, 68°C for 2.2 min (segments 1 to 4) or 1.5 min (segments 5 to 8), and a final extension of 68°C for 5 min.

Sequencing. The cDNA of the ISAV genomic segments was cloned in the pGEM T Easy vector (Promega) according to the supplier's instructions. The plasmids obtained were sequenced by standard methods (Macrogen, South Korea) using universal primers for the T7 and SP6 promoters, as well as internal primers for the segments, as described in Cottet et al. (35). The sequences were edited and analyzed with the BioEdit sequence alignment editor 7.1.3 program to generate a contig of each genomic segment of ISAV901_09, which included the universal primer sequences described above at the 3′ and 5′ ends of the UTR. The complete sequences of the eight segments of ISAV901_09 were obtained (GenBank accession numbers KM262772, KM262773, KM262774, KM262775, KM262776, KM262777, KM262778, and KM262779), and the entire viral genome was synthesized (GenScript Co.). Each segment included the SapI restriction enzyme sites at the ends to allow for cloning the viral segment without

TABLE 1 Primers for amplifying the complete eight segments of ISAV and the PB2, PB1, PA, and NP ORF from ISAV901_09

| Segment primer	Primer sequence[a] (5′ to 3′) Forward	Reverse
1a	AGCTAAGAATGGACTTTATATCAGAAAACACG	AACCTTCGAAGCCAAACAGATAG
1b	CAATATCAAGTCCGTTCGACGTGG	AGTAAAAAATGGACATTTTATTGATTAAAAGTATCGTC
2	AGCAAAGAACGCTCTTTAATAACC	AGTAAAAAATGCTCTTTTACTTATTAAAAAT
3	AGCAAAGATTGCTCAAATCCC	AGTTAAAATTGCTCTTTTCTTTATTTG
4	AGCTAAGATTGGCTGTTTCAAGA	AGTAAAAATTGGCTTTTTGGAAAA
5	AGTTAAAGATGGCTTTTCTAACAATTTT	AGTAAAAATTGGCTATTTATACAATTAATAATG
6	AGCAAAGATGGCACGATTCA	AGTAAAAAATGCACTTTTCTGTAAACG
7	AGCTAAGATTCTCCTTCTACAATGGA	AGTAAAAATTCTCCTTTTCGTTTTAAA
8	AGCAAAGATTGGCTATCTACCA	AGTAAAAAAGGCTTTTTATCTTTTG
PB2	NcoI-<u>ATGCC</u>ATGGACTTTATATCAGAAAACACGATCAGCG	XhoI-CCG<u>CTCGAG</u>AACACCATATTCATCCATAGG
PB1	SmaI-TCC<u>CCCGGG</u>AAACTCTAGTAGGTG	XhoI-CCG<u>CTCGAG</u>AACACGCTTTTTCTTCTTAATCAC
NP	MluI-CG<u>ACGCGT</u>CATGGCCGATAAAGGTATGAC	XbaI-CGC<u>TCTAGA</u>TCAAATGTCAGTGTCTTCCTC
PA	NcoI-<u>CATGCC</u>ATGGATAACCTCCGTGAATGCATAAACC	XhoI-CCG<u>CTCGAG</u>TTGGGTACTGACTGCAATTTTC

[a] The restriction sites are underlined.

incorporating additional sequences and to avoid introducing errors in the subsequent cloning into the pSS-URG vector.

Universal pSS-URG plasmid-vector design. To obtain a plasmid for the transcription of ISAV vRNA, a cassette was designed to incorporate specific elements into the pUC57 plasmid. The newly constructed vector

was named pSS-URG (for plasmid for *Salmo salar* universal reverse genetics). Figure 2A shows a scheme of all the elements included in the plasmid for the correct transcription of the vRNA. From left to right, the following elements are shown: the ITS-1 region of *Salmo salar* as a promoter (GenBank accession no. AF201312.1) (36), which contains tran-
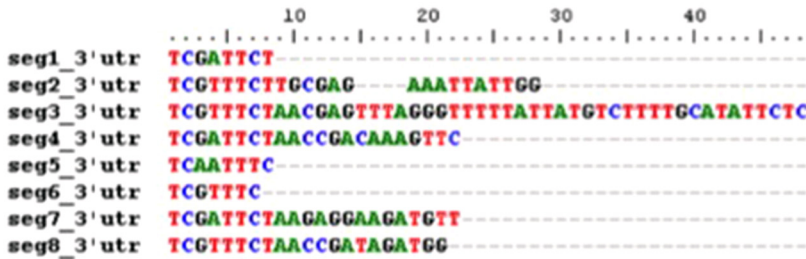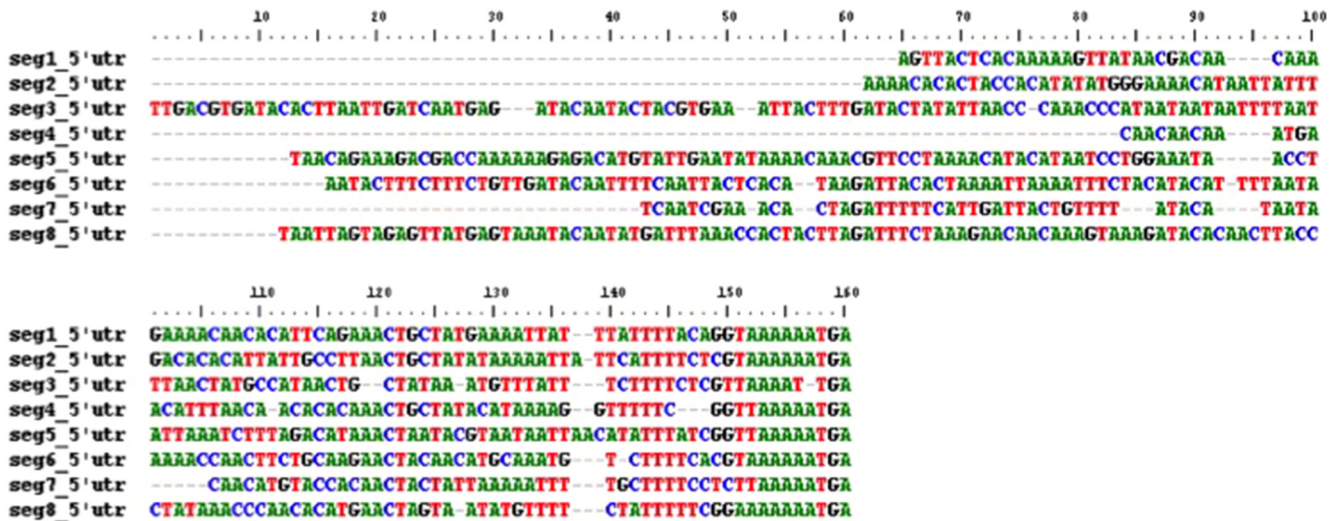

FIG 1 Alignment of 3′ and 5′ noncoding region sequences of the 8 genomic segments of the ISAV 901_09 isolate. Multiple alignments of the noncoding sequences were obtained from the cell-adapted ISAV 901_09 strain.
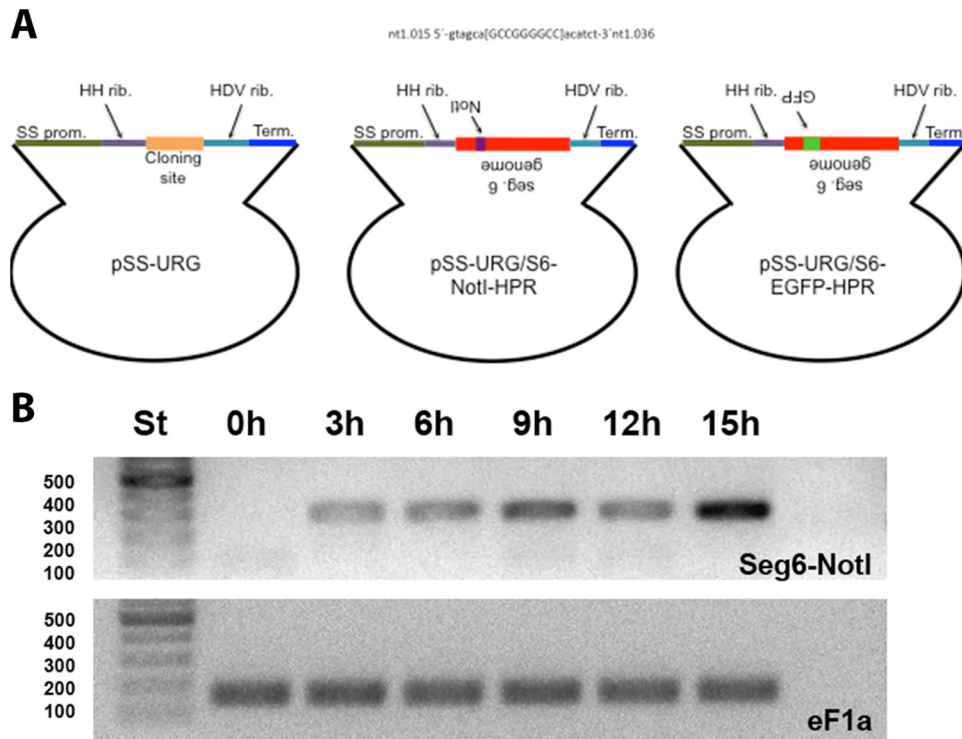
FIG 2 Generation of the universal reverse genetics system for ISAV. (A) Schematic of the design of the pSS-URG, pSS-URG/S6-NotI, and pSS-URG/S6-EGFP-HPR cassettes. The universal vector contains the sequence of the *S. salar* promoter (SS prom), the hammerhead ribozyme (HH rib), the ribozyme of the hepatitis δ virus (HDV rib), and the transcription terminator of the rabbit β-globin (Term). The pSS-URG/S6-Not and pSS-URG/S6-EGFP-HPR plasmids contain the cDNA of the antisense and inverted sequence of segment 6, which include the 5′ and 3′ UTRs and their respective modifications, the NotI restriction site, or the sequence encoding EGFP. (B) RT-PCR of segment 6-NotI-HPR from salmon ASK cells transfected with the pSS-URG/S6-NotI-HPR plasmid. RT-PCR products of segment 6 containing the NotI restriction site within the HPR of HE at different times postinfection. The RT-PCR products of salmon eF1a were used as housekeeping genes. ASK cells were transfected using Fugene 6 (Promega) with the pSS-URG/S6-NotI-HPR plasmid.

scription-promoting elements; the sequence of the hammerhead (HH) ribozyme (37); two SapI restriction sites; the hepatitis delta ribozyme (δ) (38); and the transcription terminator of rabbit beta globin. This design allows us to insert any ISAV genomic segment without incorporating additional sequences at either end of the vRNA. We then cloned the cDNA of each complete ISAV segment in this plasmid using the SapI enzyme. The plasmids obtained for each segment were named pSS-URG/1 (PB2), pSS-URG/2 (PB1), pSS-URG/3 (PA), pSS-URG/4 (NP), pSS-URG/5, pSS-URG/6, pSS-URG/7, and pSS-URG/8.

pSS-UGR/S6-NotI-HPR and pSS-UGR/S6-EGFP-HPR plasmids. Constructs containing a NotI sequence tag or EGFP were designed based on the pSS-URG/6 vector, which has the complete inverted and antisense genomic sequence (including the 3′ and 5′ UTRs) of segment 6 of ISAV 901_09. The plasmid pSS-UGR/S6-NotI-HPR, containing exactly nine nucleotides (in brackets) corresponding to the restriction site for NotI enzyme added in frame in the HPR (5′-GTAGCA[GCGGCCGCA]A-CATCT-3′ from nt 1015 to 1036) (Fig. 2A), was synthesized as described before using pUC57 as the background vector. To generate the pSS-URG/S6-EGFP-HPR plasmid, the sequence that encodes EGFP from the pEGFP-C1 plasmid (Clontech) was amplified using EGFP primers flanked by NotI restriction sites and then was introduced in frame into the NotI site of pSS-UGR/S6-NotI-HPR vector.

Generation of PB2, PB1, PA, and NP protein expression vectors. The ORFs of segments 1, 2, 3, and 4 of ISA 901_09, which encode PB2, PB1, NP, and PA, respectively (35), were amplified and cloned in the pGEM T Easy vector and then were used as templates to perform a high-fidelity PCR using *Pfx* platinum (Invitrogen) with specific primers to amplify each gene (Table 1). The pTriex3 vector (Novagen), which contains a CMV promoter, was used to clone the ORFs of PB2 and PA, using the

NcoI and XhoI restriction sites, and the PB1 ORF was cloned using the SmaI and XhoI restriction sites. The ORF encoding NP was cloned into the pCI-neo vector (Promega) using the MluI and XbaI restriction sites.

Time course analysis of ASK cells transfected with the pSS-URG/S6-NotI-HPR vector by *ex vivo* transcription assay. ASK cells were seeded at a density of $2.5 \times 10^4/cm^2$ per well in 24-well plates (SPL) in L-15 medium and cultured at 18°C until reaching 80% confluence. The cells were transfected with the pSS-URG/S6-NotI-HPR vector, using Fugene 6 (Promega), at a ratio of 1:6. The cells were incubated at 16°C for 3 h. The mixture then was removed and the cells were washed twice with phosphate-buffered saline (PBS), after which the time course of transcription was analyzed at 0, 3, 6, 9, 12, and 15 h posttransfection (hpt). At each time point, total RNA was extracted from the wells. The DNA was eliminated with RQ-DNase treatment (Promega). The RNA obtained was used to perform an RT-PCR with a primer containing the NotI restriction site (Table 2). The RT step was done with 200 U/µl of the Moloney murine leukemia virus reverse transcriptase (MMLV; New England BioLabs) in a final volume of 25 µl according to the supplier's specifications. The cDNA then was used for a PCR using the Paq5000 DNA polymerase (Agilent Technologies). The PCR was set up as recommended by the manufacturer, utilizing the S6-NotI F and the S6-5′UTR R primers at 10 µM and 10 µl of cDNA obtained during the RT step. The cycle conditions used were 95°C for 2 min; 30 cycles at 95°C for 20 s, 53°C for 20 s, and 72°C for 30 s; and a final extension of 72°C for 5 min. The PCR products were visualized by electrophoresis in a 2% agarose gel. To demonstrate that RNA inputs had similar levels, salmon eF1a was used as a housekeeping gene (39).

TABLE 2 Primers for amplifying vRNA of S6-NotI and for detection of vRNA of S6-EGFP-HPR and absolute quantification of segment 8

Primer	Sequence (5′ to 3′)
F S6-NotI	GTAGCAGCGGCCGCA
R S6-5′UTR	AGTAAAAAATGCACTTTTCTGAAACG
F S6	TGAGGGAGGTAGCATTGCAT
R S6	AAGCAACAGACAGGCTCGAT
F EGFP	CTGGAAGTTCATCTGCACCAC
R EGFP	TGCTCAGGTAGTGGTTGTC
F S8	GAAGAGTCAGGATGCCAAGACG
R S8	GAAGTCGATGAACTGCAGCGA

Modeling the HE protein of ISAV901_09 with GFP inserted within the HPR region. The HE sequence of ISAV 901_09 was obtained from the GenBank database (ADF36510.1) and then aligned with the aid of ClustalW (40) in the context of sequences of the crystal structure of the glycoprotein hemagglutinin-esterase-fusion (HEF) of influenza virus C (PDB entry 1FLC) (41). The PSIPRED prediction server for secondary structures was used to corroborate that the alignment had been done correctly (http://bioinf.cs.ucl.ac.uk/psipred/) (42). The final model of the ISAV 901_09 HE protein was obtained using the Modeler 9v9 software, which subsequently was refined and quality tested with the Anolea program. Finally, the Discovery Studio 3.5 program was used to construct the structure of HE-GFP-HPR, using the GFP crystal structure (PDB entry 1KYS). Minimization then was carried out with NAMD and CHARMM force field methods (43). Final images were obtained with the VMD program (44).

Generation of rISAV from cloned plasmids. To generate recombinant ISAV (rISAV), ASK cells were seeded at a density of 2.5×10^4 cells/cm^2 in 8- or 12-well Nunc plates (Lab-Tek II chamber slide system; Thermo Scientific) and then incubated for 72 h at 18°C. The cells were transfected as described above. To generate rISAV$^{901\_09}$, we used 250 ng of each of the expression vectors pTriex-3-PB2, pTriex-3-PB1, pTriex-3-PA, and pCI-neo-NP and 1 μg of the combined eight pSS-URG plasmids (pSS-URG/1 to pSS-URG/8). The rescue of rISAV$^{S6-NotI-HPR}$ and rISAV$^{S6-EGFP-HPR}$ was done as described above by replacing pSS-URG/6 with the respective plasmid. The cells then were incubated with 1 ml of L-15 medium for 7 days at 16°C.

Detection of rISAV$^{S6-NotI-HPR}$ in ASK cells. The supernatant from the ASK cells transfected with the plasmid mixture containing the pSS-UGR/S6-NotI-HPR vector were collected at 7 days posttransfection (dpt; passage 0 [P0] of rISAV$^{S6-NotI-HPR}$) and after passages 1 and 2. The total RNAs extracted were used to detect the vRNA of S6-NotI-HPR by RT-PCR as described above, using the specific primers for segment 6 NotI (Table 2).

Infection of ASK cells with rISAV$^{S6-EGFP-HPR}$. ASK cells were seeded as described above and grown at 16°C until reaching 90% confluence. The cells were washed twice with PBS, and blind infection passages were made with 100 μl of a 1:10 dilution of supernatant in L-15 medium without FBS but with 50 μg/ml gentamicin, either from P0 at 7 days posttransfection or from the different passages of rISAV$^{S6-EGFP-HPR}$.

The infected cells were incubated for 4 h at 16°C with the virus inocula and then washed twice with PBS, and 500 μl of L-15 medium with 10% FBS and 50 μg/ml gentamicin was added and then incubated for 7 days at 16°C. This procedure was repeated every 7 days until the fourth passage of rISAV$^{S6-EGFP-HPR}$. The supernatant from each passage was stored at −20°C until its subsequent analysis.

Analysis of rISAV$^{S6-EGFP-HPR}$ vRNA by RT-PCR and qRT-PCR. To detect rISAV$^{S6-EGFP-HPR}$, total RNA was extracted from 350 μl of supernatant from ASK cells transfected with the 12 plasmids at 7 days posttransfection (P0 of rISAV$^{S6-EGFP-HPR}$) or supernatants from the first to fourth blind passages. The RNA was treated with RNase-free DNase (Promega) before RT-PCR analysis. The primers F-UTR-S6 (Table 1), F-S6, and R-EGFP (Table 2) were used for the reverse transcription reaction with the

MMLV RT enzyme (200 U/μl; Promega) as recommended by the supplier. The GoTaq Green master mix (Promega) and the F-S6 or F-EGFP and R-S6 or R-EGFP primers were used for the PCR analysis. The cycling program used for EGFP was 95°C for 2 min; 35 cycles at 95°C for 30 s, 59.1°C for 30 s, and 72°C for 30 s; and a final extension of 72°C for 5 min. For S6 or S6-EGFP, the annealing was performed at 54°C. In all cases, each PCR product was reamplified using the same pair of primers and then was visualized in a 1% agarose gel. Real-time quantitative RT-PCR (qRT-PCR) was used to determine the vRNA copies using the absolute quantification method described by Munir and Kibenge (45), where a standard curve based on the pSS-URG/S8 plasmid was used. The qRT-PCR analysis was carried out with an Eco real-time PCR system (Illumina) and the SensiMix SYBR Hi-ROX kit (Bioline) according to the manufacturer's instructions, using the primers F-S8 and R-S8 (Table 2). The cycling conditions used for segment 8 were one cycle of 10 min at 95°C, followed by 40 cycles of 15 s at 95°C, 15 s at 60°C, and 15 s at 72°C. After the amplification, a disassociation cycle was run as 30 s at 95°C, 30 s at 55°C, and 30 s at 95°C. This procedure was carried out for the 4th passages of the recombinant virus. The results obtained were analyzed with the EcoStudy software.

Confocal microscopy. At day 7 postinfection, ASK cells infected with rISAV$^{S6-EGFP-HPR}$ from each passage of the recombinant virus were analyzed by confocal microscopy using the procedures described by Rivas-Aravena et al. (46). The fixed cells were observed with an LSM 510 (Zeiss) confocal microscope with the LSM image browser program to detect rISAV$^{S6-EGFP-HPR}$ by EGFP fluorescence. In addition, rISAV was detected by monoclonal anti-HE (BiosChile) as previously described (46).

Titration by plaque assay. ASK cells were seeded at a density of 2.5×10^4 cells/cm^2 per well in a 12-well plate (SPL) and were incubated at 16°C until reaching 100% confluence. The wild-type (WT) and recombinant ISAV strains were titrated by following the procedure described by Castillo-Cerda et al. (47).

Fluorescence quantification assay for rISAV$^{S6-EGFP-HPR}$. ASK cells were seeded at a density of 2.5×10^4 cells/cm^2 per well in a 48-well plate and incubated at 16°C until reaching 100% confluence. The virus produced during the 4th passage of rISAV$^{S6-EGFP-HPR}$ was titrated by making serial 10-fold dilutions from 10^{-1} to 10^{-6} in L-15 medium without FBS. The culture medium was removed, 400 μl of viral inoculum was added to each well, and then the wells were incubated for 4 h at 16°C to absorb the virus to the cells. The inoculum then was removed from the wells, the cells were washed twice with PBS, and L-15 medium was added. The plates were incubated for 7 days at 16°C, at which time the supernatants from the wells were analyzed and the fluorescence was quantified with a Nanoquant Infinite M200 pro instrument (Tecan, Austria) by excitation at 485 nm and emission at 535 nm. These supernatants also were used to extract total RNA and for subsequent qRT-PCR to quantify the vRNA of ISAV segment 8, as described above.

Time course of infection of ISAV901_09, rISAV$^{901\_09}$, and rISAV$^{S6/EGFP-HPR}$. ASK, RTG-2, and CSE-119 cells were infected at a multiplicity of infection (MOI) of 0.01 with the 4th passage of rISAV$^{S6/EGFP-HPR}$ or the 4th passages of rISAV$^{901\_09}$ and wild-type ISAV901_09 as controls. The time course of infection was performed using samples obtained at 0, 2, 4, and 7 days postinfection (dpi). RNA then was extracted and treated with RNase-free DNase, followed by qRT-PCR to quantify the vRNA from segment 8 to determine the copy numbers from all of the cell culture supernatants (45).

Electron microscopy. ASK cells were seeded as described above and were grown at 16°C until reaching 90% confluence. The cells were infected with 400 μl of a 1:10 dilution of the 4th passage of ISAVr$^{S6/EGFP-HPR}$, or the 4th passages of rISAV$^{901\_09}$ and WT ISAV901_09 as controls, 4 days postinfection. The cells were fixed with 2.5% glutaraldehyde in 0.1 M cacodylate buffer, pH 7.2, for 6 h at room temperature and washed with 0.1 M sodium cacodylate buffer at pH 7.2 for 18 h at 4°C. Samples were fixed with 1% aqueous osmium tetroxide for 90 min, and after soaking with distilled water, they were stained with 1% aqueous uranyl acetate for 60 min. The samples were dehydrated in a battery of acetone with increasing concentrations, 50, 70, 95 (two times), and 100% (three times), for 20
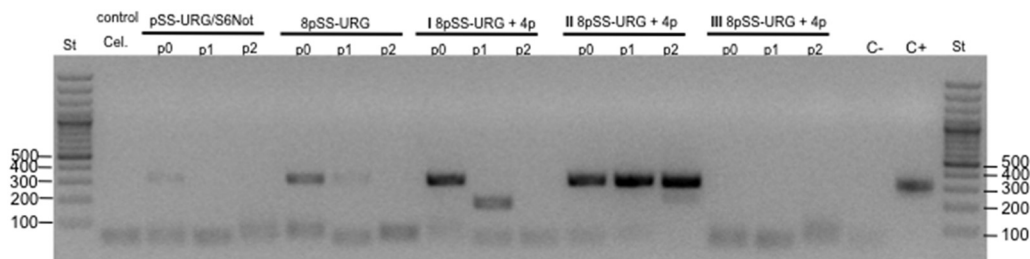
FIG 3 Rescue of plasmid-based reverse genetics system for ISAV. Shown is the detection of segment 6 with NotI from supernatants of ASK cells cotransfected with 8 pSS-URG genomic segment (segments 1 to 8) plasmids with (8pSS-URG + 4P) or without (8pSS-URG) four plasmids expressing the proteins of RNPC. The supernatant from transfected (P0) and infected cells after the first two blind passages with the rISAV were analyzed by RT-PCR 7 days postinoculation. Data show triplicate transfections (I to III) for each condition. Products were visualized by agarose electrophoresis. St, standard molecular weight marker in bp; control Cel., cells without transfection and/or infection.

min each time. The samples were embedded in epon resin-acetone at 1:1 overnight and then embedded in pure epon resin that was polymerized at 60°C for 24 h. Fine cuts (60 to 70 nm) were obtained in a Sorval MT-5000 ultramicrotome, arranged on copper grids, and stained with uranyl acetate 4% in methanol for 2 min and lead citrate for 5 min. The samples then were observed with a Philips Tecnai 12 microscope at 80 kV.

Nucleotide sequence accession numbers. The sequences of the eight segments of ISAV901_09 determined in the course of this work were deposited in GenBank under accession numbers KM262772, KM262773, KM262774, KM262775, KM262776, KM262777, KM262778, and KM262779.

RESULTS

Viral genome of the ISAV 901_09 cell culture-adapted strain. To establish an optimal genetic background to develop a reverse genetic system, we sequenced the complete genome of the ISAV 901_09 (HPR 1c) isolate, which has been adapted to cell culture in ASK cells. We first made sequence alignments of the 5′ and 3′ noncoding regions (UTR) of six ISAV isolates, two Scottish (390/98 and 982/08), one Norwegian (Glesvaer/2/90), two Canadian (NBISA01 and RPC NB 98-049), and one Chilean (ADL-PM 3205 ISAV), which showed high conservation for all genomic segments, as shown for segment 6 (see Fig. S1 in the supplemental material). These alignments allowed us to design universal primers (Table 1) that were used to amplify the complete genome of the Chilean ISAV strain 901_09 at passage 30. The length of the sequences of the eight viral genomic segments ranged from 2,267 nt to 906 nt for segments 1 to 8, respectively. The sequences of the 3′ UTRs were found to be from 7 nt in segment 6 to 48 nt in segment 3 (Fig. 1). There were no size differences compared to the previously described 3′ UTRs for the six genomes analyzed, except for the addition of one nucleotide in the 3′ UTR of segment 7 in the Chilean ISAV 901_09 isolate. The 5′ UTR also was highly conserved. The sequences of ISAV 901_09 UTRs varied from 67 nucleotides in segment 4 to 147 nt in segment 3 (Fig. 1). The alignment of the sequenced UTRs indicated that ISAV 901_09 had the same length as and a high level of similarity to the ISAV Glesvaer/2/90 strain, with sequence identity between 97% and 98%.

Generation of a universal vector for ISAV reverse genetics. To generate a vector that expresses the segments of the full-length viral RNA without additional nucleotides, we took advantage of synthetic biology and made a novel design that integrated elements used previously in the reverse genetics systems of RNA viruses, such as the hammerhead ribozyme and the ribozyme of the hepatitis delta virus (δ), together with genomic elements of the

Salmo salar species. The designed vector was called pSS-URG and was used as the backbone to develop a universal reverse genetic plasmid for ISAV.

The synthesized pSS-URG plasmid was used to subclone the eight ISAV genomic segments based on synthetic genomes that contained the SapI restriction sites (data not shown). To demonstrate the downstream generation of recombinant viruses, two genetic elements were inserted in the HPR of segment 6 of the pSS-URG/6 plasmid. We generated the vector pSS-URG/S6-NotI-HPR, which includes the NotI restriction site, and a second genetic variant that included the EGFP sequence that was named pSS-URG/S6-EGFP-HPR (Fig. 2A).

The ITS-1 region of *Salmo salar* is a functional promoter in the pSS-URG vector. In order to determine if the elements included in the vector allow for the transcription of viral RNA in salmon cells and to test the functionality of the ITS-1 region of *Salmo salar* as a promoter, we transfected ASK cells with the pSS-URG/S6-NotI-HPR plasmid in an *ex vivo* transcription assay. To determine the transcription activity of the construct, we conducted an RT-PCR to detect vRNA at 0, 3, 6, 9, 12, and 15 hpt. The reverse transcription reaction was conducted with a single primer complementary to the NotI restriction site, followed by PCR. Surprisingly, the analysis showed a PCR product as early as 3 hpt and increased transcription activity by 15 hpt (Fig. 2B). The RT-PCR products of the eF1a housekeeping gene show that the RNA input has a similar level at each time analyzed. This indicated that the cells transfected with the pSS-URG/S6-NotI-HPR plasmid generated RNA containing the NotI restriction site, confirming the ITS-1 region of *Salmo salar* as a fully functional promoter element in salmon cells.

Rescuing a fully recombinant ISAV. As has been reported for influenza virus, the minimal functional unit of the virus is the ribonucleoprotein complex (RNPC), which contains vRNA bound by multiple copies of NP and by the viral polymerase, including the PB1, PB2, and PA subunits. With the aim of establishing the RNPC in salmon cells, we cloned the ORFs of segments 1 to 4 of ISAV901_09 into a CMV expression vector (plasmids pTRiex3-PB2, pTRiex3-PB1, pTRiex3-PA, and pCI-neo-NP). To generate rISAV[S6-NotI-HPR], ASK cells were cotransfected with 12 plasmids, the four expression vectors and eight reverse genetic pSS-URG plasmids containing the genomic segments 1, 2, 3, 4, 5, 7, and 8 of ISAV901_09, as well as segment 6, containing NotI as a molecular marker (Seg6-NotI-HPR). To amplify and determine the presence of recombinant virus, two blind passages were made
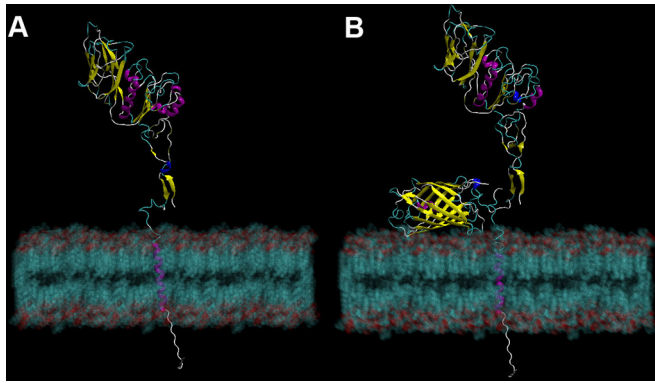
FIG 4 Crystal structure model of HE and HE-GFP chimeric proteins. (A) Cartoon representation of crystal structure model of the ISAV HE protein obtained by homology modeling using the HEF protein from influenza C virus (PDB entry 1FLC). (B) Modeling of the HE protein structure of ISAV901_09 containing EGFP inserted within HPR. Protein structures are modeled embedded in a lipid membrane. The secondary structures represent the β-sheet (yellow), alpha helix (purple), short alpha helix (blue), unstructured chain (gray), and loop chain (green/cyan).

in ASK cells infected with supernatants obtained from the transfections or the subsequent infections. The presence of vRNA from segment 6 (NotI/HPR) was detected by RT-PCR, yielding a product of the expected size (306 bp) in RNA extracted from the supernatant of the viral passages (Fig. 3), indicating the presence of infectious virus. Consequently, a fully recombinant rISAV$^{S6-NotI-HPR}$ replication-competent virus was rescued and detected in the supernatant after multiple passages. This virus produced cytopathic effect (CPE) during infection in all of the passages, resembling the plaque morphology, replication activity, and CPE seen with the WT ISAV901_09.

The HPR region of HE protein allows the introduction of EGFP. With the objective of determining whether modifications

to the HPR of the ISAV HE protein could alter the correct folding of its structure, we modeled the complete HE protein associated with the membrane. Figure 4A shows the monomer we propose of the complete HE protein embedded in a lipid membrane (of phosphatidyl oleoyl phosphatidylcholine [POPC]), which presented a relaxed structure when reaching its minimum energy using a full-atom molecular-dynamics simulation. We also modeled the HE monomer protein incorporating GFP within the HPR (HE-GFP). Analysis of the minimum of free energy of the model showed that proteins, the POPC membrane, water, and ions that participate in interactions achieve stability within 1 ns of molecular dynamics (MD) simulation. The final energy obtained was approximately $-600,000$ kcal/mol. Both models confirmed that the monomers maintain stable structures throughout the MD analysis (see Fig. S2 in the supplemental material). In both models, the stabilization of the amino and carboxyl ends of the protein can be observed above and below the membrane, respectively. The models also show that the secondary structure that maintains the HE monomer anchored to the membrane is an alpha helix from the transmembrane domain of the protein. Finally, we observed that the GFP protein did not modify the correct conformation of the HE protein when it was incorporated into the HPR, locating itself on one side of the protein stem in close contact with the upper face of the bilipid membrane.

Generation and rescue of a fluorescent rISAV$^{S6-EGFP-HPR}$. To facilitate tracing the virus in *ex vivo* assays, an rISAV containing the EGFP label was generated in ASK cells by transfection with 12 plasmids, which included the pSS-URG/S6-EGFP-HPR plasmid (segment 6) that contains EGFP within the HPR of the HE protein (rISAV$^{S6-EGFP-HPR}$) (Fig. 2A). To confirm the proper transcription of the full HE-EGFP chimeric gene produced from recombinant virus, we used RT-PCR to analyze the vRNA present in cell culture supernatants (P0) at 7 dpt. Transcription of the full vRNA was analyzed by utilizing specific primers (Table 2) directed to the EGFP gene only, segment 6 only, and the chimeric region contain-
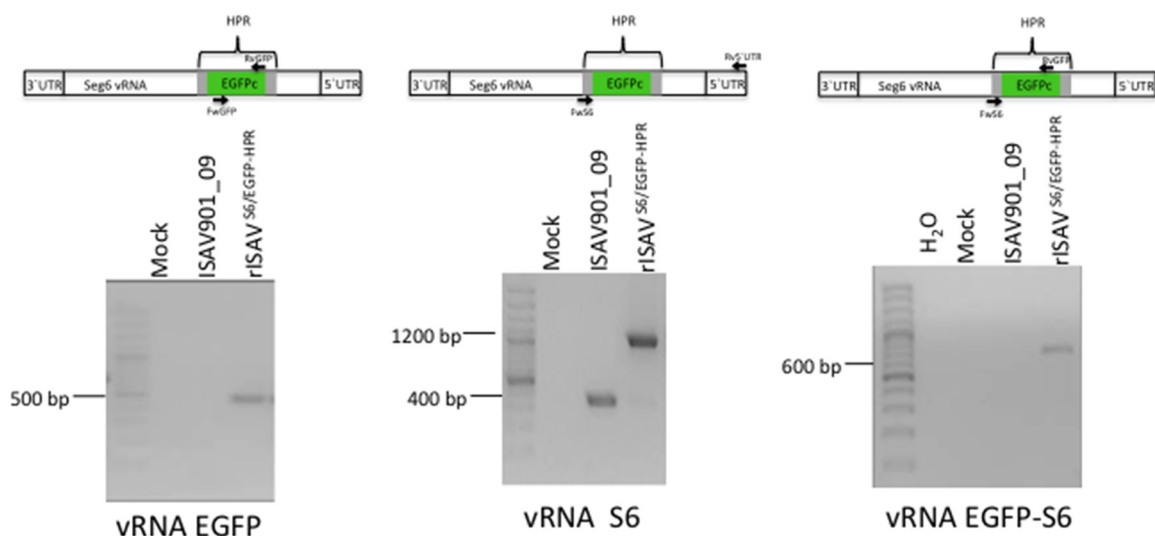

FIG 5 Transcription of HE-EGFP vRNA from rISAV. RT-PCR of RNA from supernatant of cells cotransfected with 12 plasmids, including the pSS-URG/S6-EGFP-HPR plasmid, used to generate rISAV$^{S6/EGFP-HPR}$. vRNA was amplified utilizing specific primers (Table 2) directed to the EGFP gene only (left), segment 6 only (middle), and the chimeric region containing part of both segment 6 and EGFP (right). Mock corresponds to supernatants from untransfected ASK cells, ISAV_901_09 corresponds to supernatant obtained from ASK cells infected with the WT ISAV 901 strain, and rISAV$^{S6/EGFP-HPR}$ corresponds to supernatants obtained from ASK cells infected with rISAV$^{S6/EGFP-HPR}$. Experiments were performed two times with similar results.
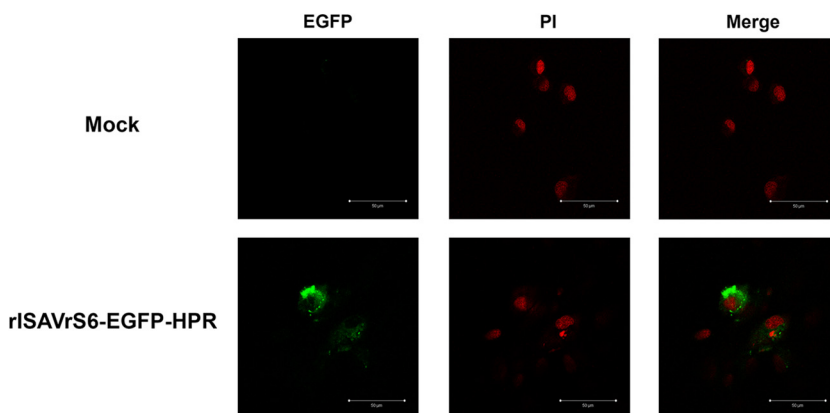
FIG 6 Expression of EGFP from the rISAV$^{S6/EGFP-HPR}$ virus. Confocal microscopy of ASK cells infected with P0 supernatant of rISAV$^{S6/EGFP-HPR}$ at 7 days postinfection. Mock corresponds to uninfected ASK cells, and rISAV$^{S6/EGFP-HPR}$ corresponds to ASK cells infected with P0 supernatant. EGFP is shown in green, and red signals show the nuclei of cells stained with propidium iodine (PI). Scale bar, 50 μm.

ing part of both segment 6 and EGFP (Fig. 5). Products of the expected sizes were obtained for the HE of the wild-type virus (~300 bp) and the recombinant virus containing the HE-EGFP protein (1,000 bp). Amplification of an internal region of the EGFP gene yielded a product of ~500 bp, which, as expected, was not present in the genome of the WT virus. A similar result was obtained for the amplification of the S6-EGFP overlapping region (~800 bp), which was obtained only for the rISAV$^{S6-EGFP-HPR}$-transfected cells.

To elucidate whether these strategies resulted in the generation of rISAV, we cotransfected ASK cells with the eight pSS-URG genomic plasmids, including the segment 6 pSS-URG/S6-EGFP-HPR plasmid, but without cotransfecting the four RNPC expression plasmids, or we cotransfected the four expression plasmids together with the pSS-URG/S6-EGFP-HPR plasmids but without the remaining seven pSS-URG genomic plasmids. vRNA from segment 6 was detected only in the supernatant of transfected ASK cells, but no vRNA was detected in the subsequent passages (data not shown). These results indicate that rISAV is rescued and detected only from supernatant of cells that were cotransfected with the 12 plasmids, confirming the importance of providing all of the components of the RNPC to achieve successful gene transcription to generate viral particles.

Infection capacity and stability of the rISAV$^{S6-EGFP-HPR}$. EGFP fluorescence was used as a reporter to determine if the supernatant of ASK cells transfected with 12 plasmids effectively contain the rISAVr$^{S6-EGFP-HPR}$ variant with characteristics of an infectious agent. ASK cells infected with this supernatant were analyzed by confocal microscopy at 7 days postinfection to determine the presence of progeny rISAV$^{S6-EGFP-HPR}$ particles. EGFP signal was visualized in infected cells, which corresponded to the first passage of rISAV$^{S6-EGFP-HPR}$ (Fig. 6), where the EGFP protein was distributed mainly in the cytoplasm and toward the plasma membrane of infected cells.

rISAV$^{S6-EGFP-HPR}$ was passaged blindly four times in ASK cells, with 7-day intervals, to assess its capacity to maintain its infectiveness and fluorescence. The supernatant from each passage was subjected to RT-PCR to detect vRNA of HE-EGFP from segment 6. Products of the correct size were obtained for EGFP, segment 6, and S6-EGFP (Fig. 7), indicating the presence of the intact and stable chimeric segment 6 containing the EGFP gene in the ana-

lyzed supernatants of all viral passages. To further confirm that each of the four passages produced infectious virus with the fluorescent label, the infected ASK cells were analyzed by confocal microscopy. The infected cells analyzed for each passage had the expected EGFP signal (Fig. 8) after each passage. This suggests that the region of the HE protein chosen to incorporate EGFP is not affected and also indicates the correct folding of both HE and EGFP. The titration of the three initial passages showed no plaques; in contrast, the fourth blind passage of the rISAV$^{S6-EGFP-HPR}$ that was titrated by plaque assay had a titer of 6.5×10^5 PFU/ml. This was equivalent to 3.63×10^6 copies/ml of segment 8 as determined by qRT-PCR. The virus obtained at this passage showed plaques with sizes similar to those obtained for WT ISAV901_09 (Fig. 9). Overall, this confirmed the generation of a stable rISAV containing a chimeric HE-GFP gene capable of infecting, replicating, and propagating after multiple passages without losing fluorescence activity.

The correlation between viral copies of ISAVr$^{S6-EGFP-HPR}$ and measured fluorescence. Given that the rISAVr$^{S6-EGFP-HPR}$ virus shows characteristics similar to those of the WT virus in ASK cells, we determined whether there was a correlation between the viral load and EGFP fluorescence in the infection supernatant produced by this rISAV. qRT-PCR analysis of rISAV$^{S6-EGFP-HPR}$ at serial dilutions and EGFP quantification established that there is a direct relationship between the fluorescence detected and viral titer of the solution. The serially passaged virus was found to have an intensity of fluorescence of 500 U/ml per titer of 1×10^6 copies/ml of segment 8 (high-dilution sample) and 2,500 U/ml per titer of 3.6×10^6 copies/ml (low-dilution sample) (Fig. 10). It is interesting that fluorescence showed linear behavior, increasing in each dilution until 2,500 U/ml, with no difference seen between the two last dilutions. In contrast, the virus titers in the number of segment 8 copies per ml showed no linear behavior in the dilution analysis caused by the variability obtained in qRT-PCR analysis. This indicates that the EGFP signal can be used as a reliable readout of infection.

Time course of rISAV$^{S6-EGFP-HPR}$ replication in salmon cell lines. To determine whether the rISAV$^{S6-EGFP-HPR}$ virus maintains the host infection range of WT ISAV901_09, we studied its capacity to infect and replicate in cells from other salmon species (i.e., RTG-2 and CSE-119 cells) and in the permissive
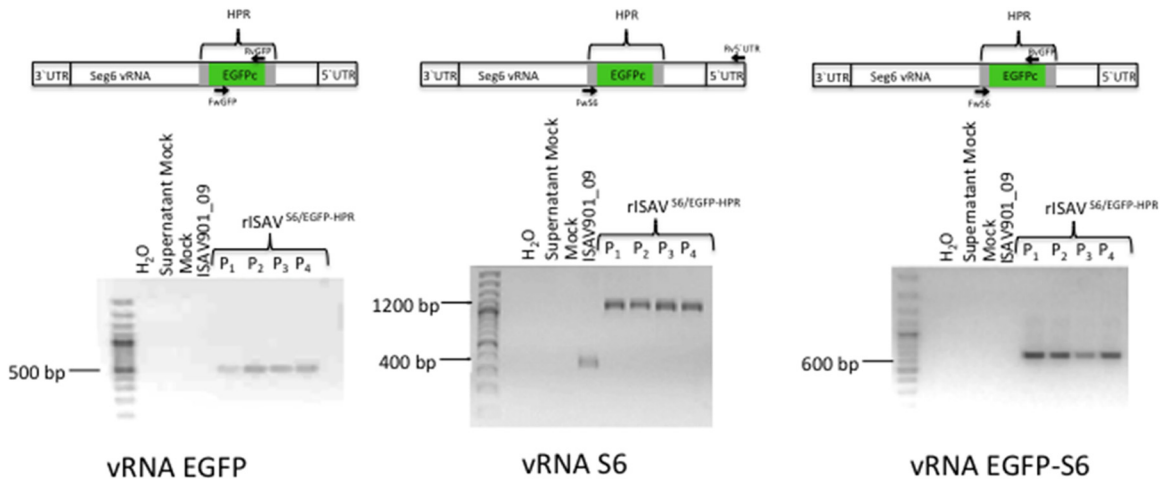
FIG 7 Rescuing of an EGFP-labeled rISAV. RNA was extracted from the supernatants from the first to fourth passages (P1 to P4) of rISAV[S6/EGFP-HPR] propagated in ASK cells for 7 days postinfection and analyzed with RT-PCR to detect chimeric vRNA utilizing specific primers (Table 2). vRNA was amplified for the EGFP gene only (left), segment 6 only (middle), or the chimeric region containing part of both segment 6 and EGFP (right). Controls include a sample lacking RNA (H$_2$O) and RNA obtained from mock transfection, which corresponds to untransfected ASK cells. ISAV_901_09 corresponds to ASK cells infected with the WT ISAV 901 strain, and rISAV[S6/EGFP-HPR] corresponds to supernatants from ASK cells infected with rISAV[S6/EGFP-HPR] for four sequential blind passages. Experiments were performed two times with similar results.

ASK cells. Infection was conducted over 7 days using passage 4 of the rISAV[S6-EGFP-HPR] virus and was compared to that using WT ISAV 901_09 and passage 4 of the rISAV[901_09] virus. vRNA from segment 8 was quantified at 0, 2, 4, and 7 dpi by qRT-PCR

in supernatants from infected cells. As expected, none of the three viruses grew in RTG-2 or CSE-119 cells (Fig. 11A and B). However, the time course of replication in ASK cells showed that initially the WT ISAV 901_09 virus replicated faster than the rISAVr[901] and rISAV[S6-EGFP-HPR] viruses. The number of copies of the recombinant viruses increased by 2 dpi, reaching ∼1 × 10^3 copies/ml, similar to the values for the WT virus. The number of copies did not increase from days 2 to 4 postinfection, but by 7 dpi the number of copies had increased by at least 10-fold, indicating that in this interval at least one replicative cycle had occurred (Fig. 11C). Thus, although the recombinant
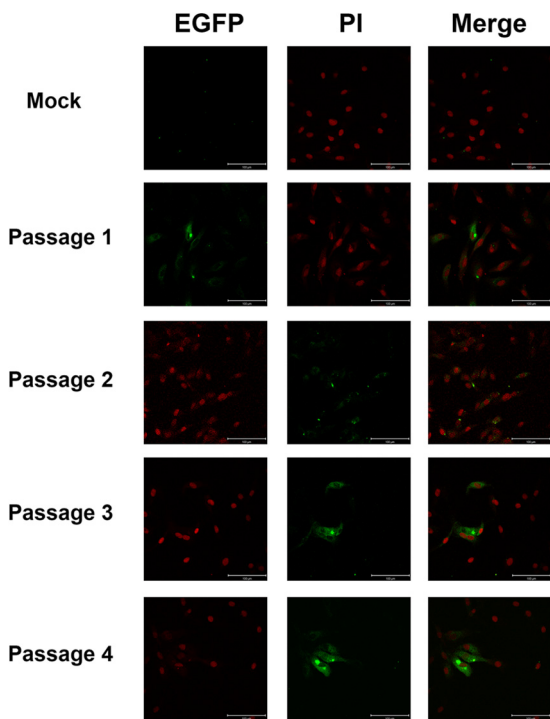

FIG 8 Confocal microscopy of ASK cells infected with rISAV[S6/EGFP-HPR] after sequential passages. Detection of EGFP at day 7 postinfection of ASK cells with supernatant from passages 1 to 4. Mock corresponds to uninfected ASK cells. Cells infected with the rISAV[S6/EGFP-HPR] during each passage are shown in green by EGFP fluorescence. Red signal shows the nuclei of cells stained with propidium iodine (PI). Scale bar, 100 μm.
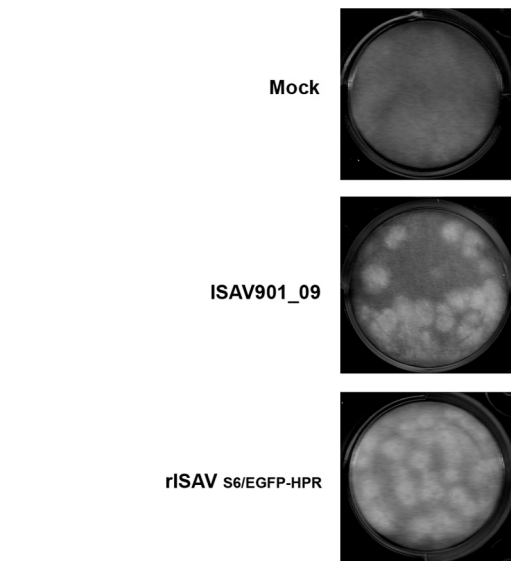

FIG 9 Plaque phenotype of rISAV[S6/EGFP-HPR]. Titration by plaque assay for rISAV[S6/EGFP-HPR] at passage 4 compared to titration of WT ISA 901_09. Infection was performed in ASK cells for 10 days. Plaques were visualized by crystal violet staining.
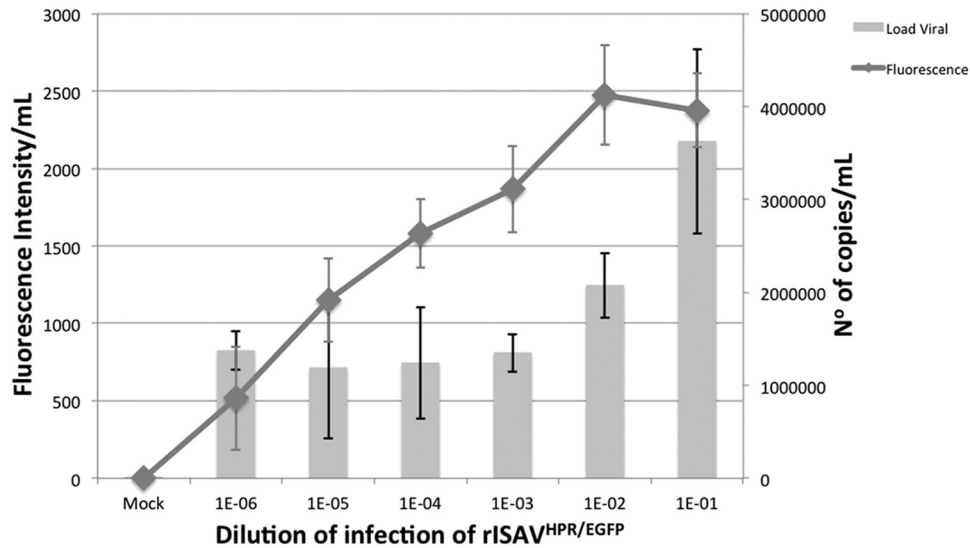
FIG 10 Relationship between fluorescence intensity and viral load of rISAV$^{S6/EGFP-HPR}$. The virus produced during the 4th passage of rISAV$^{S6-EGFP-HPR}$ was titrated by making serial 10-fold dilutions, from 10^{-1} to 10^{-6}, that were inoculated onto ASK cells. Cultures were incubated for 7 days postinfection, at which time vRNA was quantified by qRT-PCR of segment 8. The fluorescent intensity of EGFP in the supernatant was quantified by excitation at 485 nm and emission at 535 nm. Error bars correspond to the standard deviations from six samples per time point.

viruses showed slightly slower replication kinetics, these results suggest that introducing EGFP within the HPR of the HE protein does not drastically alter the replicative capacity of rISAV$^{S6-EGFP-HPR}$ in ASK cells, nor does it broaden the host infection range, at least in the *ex vivo* assays. It is worth noting that the virus titration by plaque assays from supernatants depicted in Fig. 11C showed that the level of recombinant virus had increased at 7 dpi to reach 1×10^5 PFU/ml (Fig. 11D).
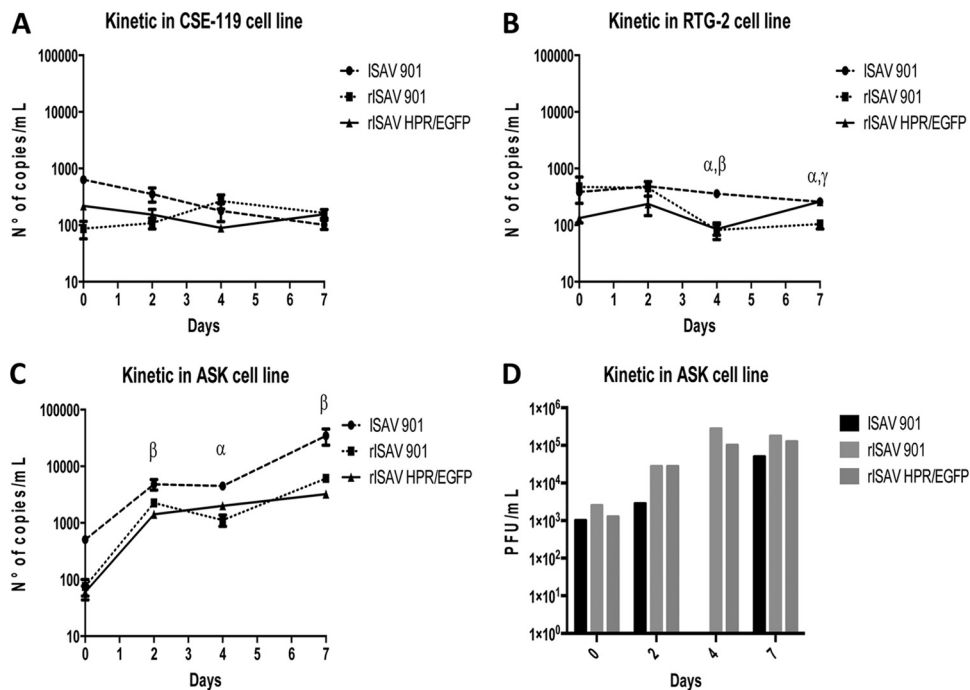

FIG 11 Time course analysis of salmon cell infection by rISAV. vRNA from segment 8 was quantified by qRT-PCR to determine the copy number from cell culture supernatants at the indicated time points postinfection with WT ISAV901_09, rISAV$^{901\_09}$, or rISAV$^{S6/EGFP-HPR}$. RTG-2 (A), CSE-119 (B), and ASK (C) cells were inoculated at an MOI of 0.01, as determined by the 50% tissue culture infectious dose. Each time point represents the averages from six replicates per time point for each virus. (D) Plaque assay results to determine the viral titer in PFU/ml from ASK cell culture supernatants shown in panel C at the indicated time points postinfection. Each time point represents the averages from two replicates per time point for each virus. Error bars represent the standard deviations. Statistical analysis was performed with nonparametric one-way analysis of variance (Kruskal-Wallis) and Dunn's multiple-comparison test. α, ISAV901_09 versus rISAV^{901}; β, ISAV901_09 versus rISAV$^{S6/EGFP-HPR}$; γ, rISAV^{901} versus rISAV$^{S6/EGFP-HPR}$.
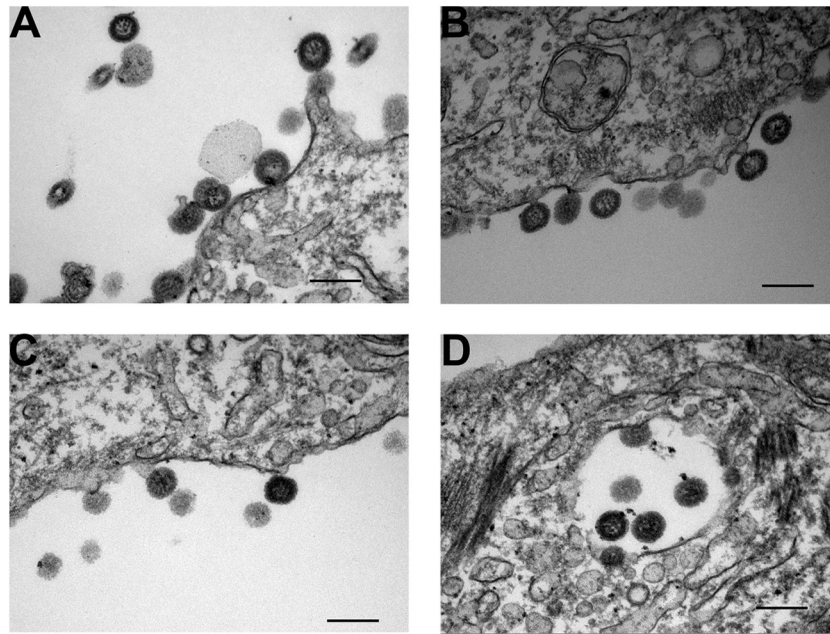
FIG 12 Electron microscopy analysis of recombinant ISAV from sectioned infected ASK cells. Shown are cytoplasmic membrane with budding ISAV particles obtained from infection with WT ISAV 901_09 (A), rISAV$^{S6\text{-}EGFP\text{-}HPR}$ (B), and rISAV$^{901–09}$ (C). (D) Endosome section showing rISAV$^{901–09}$ particles inside endosomes with some of the viral particles, which are undergoing the initial steps of membrane fusion. Scale bars, 200 nm.

Electron microscopy of recombinant ISAV. In order to determine if the molecular detection of vRNA and the results of fluorescence analysis are related to the formation of virus particles generated by our reverse genetic system, ASK cells infected with WT ISAV 901_09 and both recombinant rISAV$^{S6\text{-}EGFP\text{-}HPR}$ and rISAV$^{901–09}$ in passage 4 were visualized by transmission electron microscopy. Figure 12 shows the budding of spherical particles in the cytoplasmic membrane, with diameters of ~100 nm. The virus-like particles observed suggest the successful formation of competent virions.

DISCUSSION

Despite the severe economic losses caused by ISAV in Chile and in other salmon-farming countries (1), few studies have been conducted at the molecular biology level to gain a deep understanding of the virus-host interactions. Here, we report the development of a successful reverse genetic system for manipulating and generating rISAV from plasmid DNA. This new technology offers an important tool for understanding virulence factors and for the development of novel treatment and vaccine strategies against ISAV (48).

The fundamental requirement for developing a reverse genetic system for a virus with an RNA genome is the need for providing the entire replication machinery responsible for viral transcription and replication (26). However, unlike the viruses with a positive-sense ssRNA genome, where the genome often acts as the mRNA, viruses with a negative-sense ssRNA genome require additional considerations in the design of a rescue system. Drawing on the experience of the influenza virus field, in this study we sought to generate a plasmid-based reverse genetic system designed to deliver into cells the eight viral genomic segments together with the four RNPC proteins (49). One limitation in the development of our system was the lack of complete genome sequences publicly available for Chilean ISAV strains. In this study, we report and use the genome of an ISAV with the HPR1c genotype (ISAV 901_09), an isolate from the 2008 outbreak in Chile (35), which is adapted to cell culture.

Additionally, another consideration was to find elements of the proximal promoter for RNA polymerase I (Pol I) of *Salmo salar*. However, the full length of the IGS region is between 15 and 23 kb in the *Salmo* genus (31), making it extremely difficult to distinguish an appropriate promoter in this region, which has a high level of complexity and does not present sequence conservation among individuals of different species (30). Thus, its use in plasmid-based vectors is virtually impossible. Due to the need for using an RNA Pol I-like promoter of discrete size and the feasibility of including it in a plasmid-based construction, we focused our attention on a recently described region in the ribosomal DNA of *Salmo salar*, the ITS-1. Bioinformatic evidence using the flatworm ITS-1 region showed that it could contain transcription promoter elements with characteristics of functional ancestral sequences (32). We inferred that ITS-1 could have the same function in fish cells; therefore, we used this element as a promoter in our plasmid system. In addition, to prevent the generation of vRNA containing additional nucleotides at its ends that could affect the correct interaction between the vRNA ends and the viral polymerase, in the plasmid the cDNA template was flanked by the sequences of the hammerhead ribozyme in the 5′ end and the ribozyme of the hepatitis δ virus in the 3′ end (Fig. 2). Of interest, the simultaneous use of both ribozymes was reported recently in a replicon system in the salmon alphavirus (50). Finally, the terminator sequence of rabbit β-globin was added to the design of the cassette to ensure the correct completion of transcription (51). With the strategic incorporation of these elements in the plasmid system, the ASK cells did not require any in *trans* element to generate recombinant ISAV.

Because the universal vector designed included a promoter that was not previously described, it was necessary to determine that the pSS-URG/S6-NotI-HPR plasmid was functional and fully capable of expressing vRNA. The time course of transcription in ASK cells detected the vRNA as early as 3 hpt (Fig. 2B). RT-PCR analysis directed to the HH ribozyme and hepatitis δ ribozyme sequences did not result in an amplification product (data not shown), indicating that the RNA product was immediately auto-cleaved after transcription. Analysis using a unique primer in the RT step that recognized the NotI restriction sequence showed that the designed plasmid was functional and generated modified RNA without the need for using a restriction enzyme digestion, as was originally shown for influenza virus (52). Therefore, in this plasmid system the vRNA synthesized under the command of the ITS-1 region of *Salmo salar* generated a faithful copy of the cDNA cloned in the pSS-URG plasmid in *ex vivo* assays (Fig. 2B); thus, ITS-1 showed promoter activity similar to that of an RNA Pol I promoter (53). This successful demonstration that the ITS-1 region of vertebrates like *Salmo salar* has functional active promoter elements (data not shown) provides an important biotechnological advance to use such elements for molecular biology studies, opening a range of uses for these promoters (30). In addition, ITS-1 should be given particular attention, since it can be further exploited to develop reverse genetic systems for other RNA viruses of diverse fish species.

Since the WT ISAV901_09 strain yielded high titers in cell culture in a short time period (47), we inferred that rescue attempts using this genotype as a background would have a higher probability of generating replication-competent progeny viruses with greater efficiency in ASK cells. Thus, we generated a set of plasmids containing the 8 antisense genomic segments of the WT ISAV901_09 strain. In addition, we generated vectors to express the viral polymerase and the NP proteins of ISAV. As previously shown for influenza virus, we cotransfected 12 plasmids to provide all of the necessary genetic elements and proteins to form the eight RNPCs to initiate viral transcription and replication (26, 29).

Analysis of three transfection replicates and the two subsequent blind passages indicated that only one of the three replicates generated a stable recombinant virus (Fig. 3), most likely due to the low rate of transfection of ASK cells. An additional explanation for this could be the genetic instability of the recombinant virus after subsequent passages. Nevertheless, we could detect the vRNA containing the NotI site in subsequent passages of one rescue transfection attempt, suggesting a low rescue efficiency. To discard the possibility that this RNA was being expressed by carryover pSS-URG/S6-NotI-HPR plasmid and not from viral particles, we decided to incorporate the more robust marker, EGFP. Having the EGFP reporter protein expressed and packaged in the viral particle facilitates the detection of recombinant virus to track infections in real time. Thus, this allows the study of the distinct stages of the replication cycle, including following the infection of the virus in cell culture and complete organisms (54), as has been shown for recombinant influenza viruses labeled with GFP (54, 55).

Segment 6, encoding HE protein, is one of the major and most antigenic proteins of the virus (56), and it retains functionality despite a high variation in the length of its stalk due to the existence of a highly polymorphic region. The HPR can contain natural deletions, which have been related to the acquisition of an *in*

vivo virulent phenotype, possibly derived from an ancestral avirulent strain, HPR0 (20). Additionally, it has been shown previously through the expression of recombinant proteins that variations in these zones do not affect the function of HE (17). Consequently, we proposed that the HPR has the necessary plasticity to make modifications that will not be detrimental to the viability of the virus and its infection and replication capacity, and that its modification has a low probability of altering the function and structure of this protein. Indeed, modeling the monomer of the HE protein embedded in a lipidic bilayer allowed us to determine that the HPR would be a loop without defined secondary structure (Fig. 4). Based on its sequence plasticity, we hypothesized that the HPR could support the insertion of a larger structure, like that of EGFP. The modeling of the chimeric HE-GFP protein showed a structure as stable as that of the wild-type HE monomer (Fig. 4; also see Fig. S2 in the supplemental material), suggesting that this region can be modified without greatly altering the main structure and function of the protein and its association with the viral membrane. Thus, we took advantage of the NotI restriction site and cloned the EGFP coding sequence within the HPR of segment 6 of ISAV. Our approach allowed us to detect the rISAV genome containing the EGFP gene in the supernatant of transfected cells (Fig. 5). We could not detect the rISAV genome in the supernatants of the cells in which the four vectors expressing the proteins of the RNPC were excluded from the transfection mix. These results strongly suggest that the putative functions proposed for the proteins encoded by segments 1, 2, and 4 are the subunits of the viral polymerase (57). Moreover, detection of EGFP vRNA within segment 6 in cell supernatant (Fig. 5) also suggested that this vRNA could be packaged in the viral particle, as was later confirmed by electron microscopy analysis of the progeny recombinant virus (Fig. 12).

To provide additional proof that we had obtained an infectious rISAV labeled with EGFP, we analyzed infected cells by confocal microscopy. EGFP signal (Fig. 6) was detected in cells infected with the EGFP rISAV present in cell supernatants, suggesting that the recombinant vRNA detected forms part of a viral particle. Moreover, this suggests that it possesses functional HE-EGFP, capable of interacting with the cell receptor and infecting ASK cells, as well as showing the characteristic cytopathic effect (e.g., foci of fused cells) seen with the WT ISAV (56, 58). Thanks to the β barrel structure of GFP and its fluorescent capacity, this protein has been fused to other viral proteins without interfering in its correct folding and consequently permitting the formation of native viral capsids. An example of this was reported earlier for the hepatitis B virus, where the fusion of GFP with HBcAg does not interfere with the formation of virus-like particles (59). Our data showed that the EGFP rISAV generated is stable after four successive passages in cell culture without losing its modification (Fig. 7). Florescent microcopy of cells infected at each passage indicated an efficient infection, as revealed by an increase in the EGFP signal (Fig. 8), confirming that for at least the first four passages, the rISAV^S6/EGFP-HPR virus remained stable and infectious. It is noteworthy that the distribution of EGFP from rISAV^S6/EGFP-HPR localized mainly in the form of vesicles at the perinuclear region toward the plasma membrane and widely distributed in the cytoplasm (Fig. 8), which mimics the pattern of localization of the WT HE during viral infection in cell culture (56, 58). Furthermore, colocalization of the HE protein with EGFP signal (see Fig. S4 in the supplemental material) also

demonstrated that the chimeric protein remained functional as part of the viral particle. Altogether, these findings indicate that the region of the HE protein chosen to incorporate EGFP has the plasticity to incorporate exogenous domains without altering the correct protein folding and consequently the functionality of the HE protein in this recombinant virus. These results also suggest that our plasmid system can be used to introduce additional peptides or proteins, which can be a valuable approach in the development of multiepitope vaccines, as has been described for an adenoviral vector that was used to create a chimeric protein expressing the mammalian reovirus σ1 protein at the end of the fiber protein domain (60).

rISAV$^{S6/EGFP-HPR}$ is infectious and mirrors the capacity of the WT ISAV901_09 strain to produce cytopathic effects in ASK cells. The fourth passage of the recombinant virus was capable of generating plaques and grew to a titer of 6.5×10^5 PFU/ml (Fig. 9), similar to the titers typically obtained for WT ISAV901_09 (47). Of note, qRT-PCR indicated a titer of 3.63×10^6 copies of segment 8/ml, which suggests that not all of the replicative viral particles generated in the cell become infectious viruses, a phenomenon described previously for the WT ISAV (47). Nonetheless, analysis of a known concentration of rISAV$^{S6/EGFP-HPR}$ established that there is a close relationship between the quantity of viral genomes and the quantified fluorescent units (Fig. 10). Therefore, direct quantitation of the EGFP signal provides a valuable tool to study inhibitors of entry and replication kinetics, as has been previously reported for influenza virus using viruses that express GFP to assess antiviral efficacy (61, 62).

Given the characteristics of the ISAV with the HPR0 genotype, which contains a full-length HPR region, it is catalogued as avirulent and incapable of replicating in other commonly used cell cultures (48). For instance, it has been shown that ISAV 901_09 virus can infect SHK-1 and ASK cells (47, 63). However, other ISAV strains with different HPR lengths can be isolated from diverse cell lines (4, 8, 63–65). Thus, we reasoned that the incorporation of a large sequence within the HPR of segment 6 affects its infection capacity in cell culture; therefore, it was important to assess the capacity of the rISAV$^{S6-EGFP-HPR}$ virus to replicate in different cell lines. Time-course analyses of infection in CSE-119 (Pacific salmon) and RTG-2 (rainbow trout) cells showed no replication of any of the viruses studied (e.g., WT ISAV 901_09, rISAV$^{901\_09}$, or rISAV$^{S6/EGFP-HPR}$). In contrast, the three viruses infected ASK cells and had equivalent replication kinetics and viral titers after 7 days (Fig. 11C). rISAVr$^{S6-EGFP-HPR}$ replicated to levels comparable to those of the WT ISAV 901_09 virus, as assessed by plaque assay during 7 dpi (Fig. 11D). Overall, these findings suggest that a modification of the HE genome within the HPR is not detrimental to the replicative capacity of the recombinant viruses, which retain the infection capacity of the WT virus, at least in *ex vivo* conditions.

In summary, we developed a novel reverse genetics system based on a functional plasmid containing a novel promoter derived from ITS-1 that is capable of expressing intact genomic vRNA, allowing the full rescue of infectious rISAV. This novel platform also allowed us to modify the genome of the virus, taking advantage of the plasticity of the HPR region of the HE protein to generate a stable infectious virus expressing EGFP with characteristics resembling those of the WT virus. This is a major advance in the field and has enormous potential for studying molecular processes and functions, host-virus interactions, and still-unknown

virulence factors that are critical to better understanding the molecular biology of ISAV and to develop new antiviral therapies and more effective vaccines, which is of paramount importance for salmon-producing countries.

REFERENCES

1. **Asche F, Hansen H, Tveteras R, Tveterås S.** 2009. The salmon disease crisis in Chile. Mar Resour Econ **24:**405–411. http://dx.doi.org/10.5950/0738-1360-24.4.405.
2. **Godoy MG, Aedo A, Kibenge MJ, Groman DB, Yason CV, Grothusen H, Lisperguer A, Calbucura M, Avendano F, Imilan M, Jarpa M, Kibenge FS.** 2008. First detection, isolation and molecular characterization of infectious salmon anaemia virus associated with clinical disease in farmed Atlantic salmon (Salmo salar) in Chile. BMC Vet Res **4:**28. http://dx.doi.org/10.1186/1746-6148-4-28.
3. **Thoroud K, Djupvik HO.** 1988. Infectious salmon anemia in Atlantic salmon (salmo salar L.). Bull Eur Assoc Fish Pathol **8:**109–111.
4. **Bouchard D, Keleher W, Opitz HM, Blake S, Edwards KC, Nicholson BL.** 1999. Isolation of infectious salmon anemia virus (ISAV) from Atlantic salmon in New Brunswick, Canada. Dis Aquat Organ **35:**131–137. http://dx.doi.org/10.3354/dao035131.
5. **Rowley HMCSJ, Curran WL, Turnbull T, Bryson DG.** 1999. Isolation of infectious salmon anaemia virus (ISAV) from Scottish farmed Atlantic salmon, Salmo salar L. J Fish Dis **22:**483–487.
6. **Lovely JE, Dannevig BH, Falk K, Hutchin L, MacKinnon AM, Melville KJ, Rimstad E, Griffiths SG.** 1999. First identification of infectious salmon anaemia virus in North America with haemorrhagic kidney syndrome. Dis Aquat Organ **35:**145–148. http://dx.doi.org/10.3354/dao035145.
7. **Kibenge FS, Garate ON, Johnson G, Arriagada R, Kibenge MJ, Wadowska D.** 2001. Isolation and identification of infectious salmon anaemia virus (ISAV) from Coho salmon in Chile. Dis Aquat Organ **45:**9–18. http://dx.doi.org/10.3354/dao045009.
8. **Dannevig BH, Falk K, Namork E.** 1995. Isolation of the causal virus of infectious salmon anaemia (ISA) in a long-term cell line from Atlantic salmon head kidney. J Gen Virol **76**(Part 6):1353–1359. http://dx.doi.org/10.1099/0022-1317-76-6-1353.
9. **Krossoy B, Nilsen F, Falk K, Endresen C, Nylund A.** 2001. Phylogenetic analysis of infectious salmon anaemia virus isolates from Norway, Canada and Scotland. Dis Aquat Organ **44:**1–6. http://dx.doi.org/10.3354/dao044001.
10. **Merour E, LeBerre M, Lamoureux A, Bernard J, Bremont M, Biacchesi S.** 2011. Completion of the full-length genome sequence of the infectious salmon anemia virus, an aquatic orthomyxovirus-like, and characterization of mAbs. J Gen Virol **92:**528–533. http://dx.doi.org/10.1099/vir.0.027417-0.
11. **Rimstad E, Mjaaland S.** 2002. Infectious salmon anaemia virus. APMIS **110:**273–282. http://dx.doi.org/10.1034/j.1600-0463.2002.100401.x.
12. **Palese P, Shaw ML.** 2007. Orthomyxoviridae: the viruses and their replication. *In* Knipe DM, Howley PM, Griffin DE, Lamb RA, Martin MA, Roizman B, Straus SE (ed), Fields virology, 5th ed. Lippincott Williams & Wilkins, Philadelphia, PA.
13. **Aspehaug V, Falk K, Krossoy B, Thevarajan J, Sanders L, Moore L, Endresen C, Biering E.** 2004. Infectious salmon anemia virus (ISAV)

genomic segment 3 encodes the viral nucleoprotein (NP), an RNA-binding protein with two monopartite nuclear localization signals (NLS). Virus Res **106**:51–60. http://dx.doi.org/10.1016/j.virusres.2004.06.001.

14. **Neumann G, Brownlee GG, Fodor E, Kawaoka Y.** 2004. Orthomyxovirus replication, transcription, and polyadenylation. Curr Top Microbiol Immunol **283**:121–143. http://dx.doi.org/10.1007/978-3-662-06099-5_4.

15. **Aspehaug V, Mikalsen AB, Snow M, Biering E, Villoing S.** 2005. Characterization of the infectious salmon anemia virus fusion protein. J Virol **79**:12544–12553. http://dx.doi.org/10.1128/JVI.79.19.12544-12553.2005.

16. **Hellebo A, Vilas U, Falk K, Vlasak R.** 2004. Infectious salmon anemia virus specifically binds to and hydrolyzes 4-O-acetylated sialic acids. J Virol **78**:3055–3062. http://dx.doi.org/10.1128/JVI.78.6.3055-3062.2004.

17. **Muller A, Solem ST, Karlsen CR, Jorgensen TO.** 2008. Heterologous expression and purification of the infectious salmon anemia virus hemagglutinin esterase. Protein Expr Purif **62**:206–215. http://dx.doi.org/10.1016/j.pep.2008.08.006.

18. **Devold M, Falk K, Dale B, Krossoy B, Biering E, Aspehaug V, Nilsen F, Nylund A.** 2001. Strain variation, based on the hemagglutinin gene, in Norwegian ISA virus isolates collected from 1987 to 2001: indications of recombination. Dis Aquat Organ **47**:119–128. http://dx.doi.org/10.3354/dao047119.

19. **Christiansen DH, Ostergaard PS, Snow M, Dale OB, Falk K.** 2011. A low-pathogenic variant of infectious salmon anemia virus (ISAV-HPR0) is highly prevalent and causes a nonclinical transient infection in farmed Atlantic salmon (Salmo salar L.) in the Faroe Islands. J Gen Virol **92**:909–918. http://dx.doi.org/10.1099/vir.0.027094-0.

20. **Kibenge FS, Godoy MG, Wang Y, Kibenge MJ, Gherardelli V, Mansilla S, Lisperger A, Jarpa M, Larroquete G, Avendano F, Lara M, Gallardo A.** 2009. Infectious salmon anaemia virus (ISAV) isolated from the ISA disease outbreaks in Chile diverged from ISAV isolates from Norway around 1996 and was disseminated around 2005, based on surface glycoprotein gene sequences. Virol J **6**:88. http://dx.doi.org/10.1186/1743-422X-6-88.

21. **Nylund A, Plarre H, Karlsen M, Fridell F, Ottem KF, Bratland A, Saether PA.** 2007. Transmission of infectious salmon anaemia virus (ISAV) in farmed populations of Atlantic salmon (Salmo salar). Arch Virol **152**:151–179. http://dx.doi.org/10.1007/s00705-006-0825-9.

22. **Mjaaland S, Hungnes O, Teig A, Dannevig BH, Thorud K, Rimstad E.** 2002. Polymorphism in the infectious salmon anemia virus hemagglutinin gene: importance and possible implications for evolution and ecology of infectious salmon anemia disease. Virology **304**:379–391. http://dx.doi.org/10.1006/viro.2002.1658.

23. **Cunningham CO, Gregory A, Black J, Simpson I, Raynard RS.** 2002. A novel variant of the infectious salmon anaemia virus (ISAV) haemagglutinin gene suggests mechanisms for virus diversity. Bull Eur Assoc Fish Pathol **22**:366–374.

24. **McBeath AJ, Collet B, Paley R, Duraffour S, Aspehaug V, Biering E, Secombes CJ, Snow M.** 2006. Identification of an interferon antagonist protein encoded by segment 7 of infectious salmon anaemia virus. Virus Res **115**:176–184. http://dx.doi.org/10.1016/j.virusres.2005.08.005.

25. **Garcia-Rosado E, Markussen T, Kileng O, Baekkevold ES, Robertsen B, Mjaaland S, Rimstad E.** 2008. Molecular and functional characterization of two infectious salmon anaemia virus (ISAV) proteins with type I interferon antagonizing activity. Virus Res **133**:228–238. http://dx.doi.org/10.1016/j.virusres.2008.01.008.

26. **Garcia-Sastre A, Palese P.** 1993. Genetic manipulation of negative-strand RNA virus genomes. Annu Rev Microbiol **47**:765–790. http://dx.doi.org/10.1146/annurev.mi.47.100193.004001.

27. **Fodor E, Devenish L, Engelhardt OG, Palese P, Brownlee GG, Garcia-Sastre A.** 1999. Rescue of influenza A virus from recombinant DNA. J Virol **73**:9679–9682.

28. **Hoffmann E, Webster RG.** 2000. Unidirectional RNA polymerase I-polymerase II transcription system for the generation of influenza A virus from eight plasmids. J Gen Virol **81**:2843–2847.

29. **Neumann G, Watanabe T, Ito H, Watanabe S, Goto H, Gao P, Hughes M, Perez DR, Donis R, Hoffmann E, Hobom G, Kawaoka Y.** 1999. Generation of influenza A viruses entirely from cloned cDNAs. Proc Natl Acad Sci U S A **96**:9345–9350. http://dx.doi.org/10.1073/pnas.96.16.9345.

30. **Comai L.** 2004. Mechanism of RNA polymerase I transcription. Adv Protein Chem **67**:123–155. http://dx.doi.org/10.1016/S0065-3233(04)67005-7.

31. **Castro J, Sanchez L, Martinez P, Lucchini SD, Nardi I.** 1997. Molecular analysis of a NOR site polymorphism in brown trout (Salmo trutta): organization of rDNA intergenic spacers. Genome **40**:916–922. http://dx.doi.org/10.1139/g97-118.

32. **Van Herweden L, Caley MJ, Blair D.** 2003. Regulatory motifs are present in the ITS1 of some flatworm species. J Exp Zool **296B**:80–86. http://dx.doi.org/10.1002/jez.b.8.

33. **Fourrier M, Heuser S, Munro E, Snow M.** 2011. Characterization and comparison of the full 3′ and 5′ untranslated genomic regions of diverse isolates of infectious salmon anaemia virus by using a rapid and universal method. J Virol Methods **174**:136–143. http://dx.doi.org/10.1016/j.jviromet.2011.03.023.

34. **Kulshreshtha V, Kibenge M, Salonius K, Simard N, Riveroll A, Kibenge F.** 2010. Identification of the 3′ and 5′ terminal sequences of the 8 RNA genome segments of European and North American genotypes of infectious salmon anemia virus (an orthomyxovirus) and evidence for quasi-species based on the non-coding sequences of transcripts. Virol J **7**:338. http://dx.doi.org/10.1186/1743-422X-7-338.

35. **Cottet L, Cortez-San Martin M, Tello M, Olivares E, Rivas-Aravena A, Vallejos E, Sandino AM, Spencer E.** 2010. Bioinformatic analysis of the genome of infectious salmon anemia virus associated with outbreaks with high mortality in Chile. J Virol **84**:11916–11928. http://dx.doi.org/10.1128/JVI.01202-10.

36. **Reed KM, Hackett JD, Phillips RB.** 2000. Comparative analysis of intra-individual and inter-species DNA sequence variation in salmonid ribosomal DNA cistrons. Gene **249**:115–125. http://dx.doi.org/10.1016/S0378-1119(00)00156-6.

37. **Penchovsky R, Breaker RR.** 2005. Computational design and experimental validation of oligonucleotide-sensing allosteric ribozymes. Nat Biotechnol **23**:1424–1433. http://dx.doi.org/10.1038/nbt1155.

38. **Puerta-Fernandez E, Romero-Lopez C, Barroso-del Jesus A, Berzal-Herranz A.** 2003. Ribozymes: recent advances in the development of RNA tools. FEMS Microbiol Rev **27**:75–97. http://dx.doi.org/10.1016/S0168-6445(03)00020-2.

39. **Reyes-Cerpa S, Reyes-López FE, Toro-Ascuy D, Ibañez J, Maisey K, Sandino AM, Imarai M.** 2012. IPNV modulation of pro and anti-inflammatory cytokine expression in Atlantic salmon might help the establishment of infection and persistence. Fish Shellfish Immunol **32**:291–300. http://dx.doi.org/10.1016/j.fsi.2011.11.018.

40. **Thompson JD, Higgins DG, Gibson TJ.** 1994. CLUSTAL W: improving the sensitivity of progressive multiple sequence alignment through sequence weighting, position-specific gap penalties and weight matrix choice. Nucleic Acids Res **22**:4673–4680. http://dx.doi.org/10.1093/nar/22.22.4673.

41. **Castro-Nallar E, Cortez-San Martin M, Mascayano C, Molina C, Crandall KA.** 2011. Molecular phylodynamics and protein modeling of infectious salmon anemia virus (ISAV). BMC Evol Biol **11**:349. http://dx.doi.org/10.1186/1471-2148-11-349.

42. **Jones DT.** 1999. Protein secondary structure prediction based on position-specific scoring matrices. J Mol Biol **292**:195–202. http://dx.doi.org/10.1006/jmbi.1999.3091.

43. **Brooks BR, Olafson BRBD, States DJ, Swaminathan S, Karplus M.** 1983. CHARMM: a program for macromolecular energy, minimization, and dynamics calculations. J Comput Chem **4**:187–217. http://dx.doi.org/10.1002/jcc.540040211.

44. **Guex N, Peitsch MC.** 1997. SWISS-MODEL and the Swiss-PdbViewer: an environment for comparative protein modeling. Electrophoresis **18**:2714–2723. http://dx.doi.org/10.1002/elps.1150181505.

45. **Munir K, Kibenge FS.** 2004. Detection of infectious salmon anaemia virus by real-time RT-PCR. J Virol Methods **117**:37–47. http://dx.doi.org/10.1016/j.jviromet.2003.11.020.

46. **Rivas-Aravena A, Vallejos-Vidal E, Cortez-San Martin M, Reyes-Lopez F, Tello M, Mora P, Sandino AM, Spencer E.** 2011. Inhibitory effect of a nucleotide analog on infectious salmon anemia virus infection. J Virol **85**:8037–8045. http://dx.doi.org/10.1128/JVI.00533-11.

47. **Castillo-Cerda MT, Cottet L, Toro-Ascuy D, Spencer E, Cortez-San Martin M.** 2013. Development of plaque assay for Chilean infectious salmon anaemia virus, application for virus purification and titration in salmon ASK cells. J Fish Dis **37**:989–995. http://dx.doi.org/10.1111/jfd.12198.

48. **Godoy MG, Kibenge MJ, Suarez R, Lazo E, Heisinger A, Aguinaga J, Bravo D, Mendoza J, Llegues KO, Avendano-Herrera R, Vera C, Mardones F, Kibenge FS.** 2013. Infectious salmon anaemia virus (ISAV) in Chilean Atlantic salmon (Salmo salar) aquaculture: emer-

gence of low pathogenic ISAV-HPR0 and re-emergence of virulent ISAV-HPR: HPR3 and HPR14. Virol J **10**:344. http://dx.doi.org/10.1186/1743-422X-10-344.

49. **Coloma R, Valpuesta JM, Arranz R, Carrascosa JL, Ortin J, Martin-Benito J.** 2009. The structure of a biologically active influenza virus ribonucleoprotein complex. PLoS Pathog **5**:e1000491. http://dx.doi.org/10.1371/journal.ppat.1000491.

50. **Wolf A, Hodneland K, Frost P, Braaen S, Rimstad E.** 2013. A hemagglutinin-esterase-expressing salmonid alphavirus replicon protects Atlantic salmon (Salmo salar) against infectious salmon anemia (ISA). Vaccine **31**:661–669. http://dx.doi.org/10.1016/j.vaccine.2012.11.045.

51. **Lanoix J, Acheson NH.** 1988. A rabbit beta-globin polyadenylation signal directs efficient termination of transcription of polyomavirus DNA. EMBO J **7**:2515–2522.

52. **Pleschka S, Jaskunas R, Engelhardt OG, Zurcher T, Palese P, Garcia-Sastre A.** 1996. A plasmid-based reverse genetics system for influenza A virus. J Virol **70**:4188–4192.

53. **Zobel A, Neumann G, Hobom G.** 1993. RNA polymerase I catalysed transcription of insert viral cDNA. Nucleic Acids Res **21**:3607–3614. http://dx.doi.org/10.1093/nar/21.16.3607.

54. **Manicassamy B, Manicassamy S, Belicha-Villanueva A, Pisanelli G, Pulendran B, Garcia-Sastre A.** 2010. Analysis of in vivo dynamics of influenza virus infection in mice using a GFP reporter virus. Proc Natl Acad Sci U S A **107**:11531–11536. http://dx.doi.org/10.1073/pnas.0914994107.

55. **Kittel C, Sereinig S, Ferko B, Stasakova J, Romanova J, Wolkerstorfer A, Katinger H, Egorov A.** 2004. Rescue of influenza virus expressing GFP from the NS1 reading frame. Virology **324**:67–73. http://dx.doi.org/10.1016/j.virol.2004.03.035.

56. **Falk K, Aspehaug V, Vlasak R, Endresen C.** 2004. Identification and characterization of viral structural proteins of infectious salmon anemia virus. J Virol **78**:3063–3071. http://dx.doi.org/10.1128/JVI.78.6.3063-3071.2004.

57. **Cottet L, Rivas-Aravena A, Cortez-San Martin M, Sandino AM, Spencer E.** 2011. Infectious salmon anemia virus—genetics and pathogenesis. Virus Res **155**:10–19. http://dx.doi.org/10.1016/j.virusres.2010.10.021.

58. **Rolland JB, Bouchard D, Winton JR.** 2003. Improved diagnosis of infectious salmon anaemia virus by use of a new cell line derived from Atlantic salmon kidney tissue, p 63–68. *In* Proceedings of the International Response to Infectious Salmon Anemia: Prevention, Control, and Eradication. U.S. Department of Agriculture, Washington, DC.

59. **Kratz PA, Bottcher B, Nassal M.** 1999. Native display of complete foreign protein domains on the surface of hepatitis B virus capsids. Proc Natl Acad Sci U S A **96**:1915–1920. http://dx.doi.org/10.1073/pnas.96.5.1915.

60. **Mercier GT, Campbell JA, Chappell JD, Stehle T, Dermody TS, Barry MA.** 2004. A chimeric adenovirus vector encoding reovirus attachment protein sigma1 targets cells expressing junctional adhesion molecule 1. Proc Natl Acad Sci U S A **101**:6188–6193. http://dx.doi.org/10.1073/pnas.0400542101.

61. **Kim JI, Park S, Lee I, Lee S, Shin S, Won Y, Hwang MW, Bae JY, Heo J, Hyun HE, Jun H, Lim SS, Park MS.** 2012. GFP-expressing influenza A virus for evaluation of the efficacy of antiviral agents. J Microbiol **50**:359–362. http://dx.doi.org/10.1007/s12275-012-2163-9.

62. **Sutton TC, Obadan A, Lavigne J, Chen H, Li W, Perez DR.** 2014. Genome rearrangement of influenza virus for anti-viral drug screening. Virus Res **189**:14–23. http://dx.doi.org/10.1016/j.virusres.2014.05.003.

63. **Rolland JB, Bouchard D, Coll J, Winton JR.** 2005. Combined use of the ASK and SHK-1 cell lines to enhance the detection of infectious salmon anemia virus. J Vet Diagn Investig **17**:151–157. http://dx.doi.org/10.1177/104063870501700209.

64. **Devold M, Krossoy B, Aspehaug V, Nylund A.** 2000. Use of RT-PCR for diagnosis of infectious salmon anaemia virus (ISAV) in carrier sea trout Salmo trutta after experimental infection. Dis Aquat Organ **40**:9–18. http://dx.doi.org/10.3354/dao040009.

65. **Falk K, Namork E, Dannevig BH.** 1998. Characterization and applications of a monoclonal antibody against infectious salmon anaemia virus. Dis Aquat Organ **34**:77–85. http://dx.doi.org/10.3354/dao034077.